JACS
JOURNAL OF THE AMERICAN CHEMICAL SOCIETY

Communication

pubs.acs.org/JACS

Boron Nitride Nanosheet on Gold as an Electrocatalyst for Oxygen Reduction Reaction: Theoretical Suggestion and Experimental Proof

Kohei Uosaki,*[,†,‡,§] Ganesan Elumalai,[†,‡] Hidenori Noguchi,[†,‡,§] Takuya Masuda,[‡] Andrey Lyalin,[∥,¶] Akira Nakayama,[†,∥,⊥,+] and Tetsuya Taketsugu[†,∥,⊥]

[†]Graduate School of Chemical Sciences and Engineering, Hokkaido University, Sapporo 060-0810, Japan

[‡]Global Research Center for Environment and Energy based on Nanomaterials Science (GREEN), National Institute for Materials Science (NIMS), Tsukuba 305-0044, Japan

[§]International Center for Materials Nanoarchitectonics (WPI-MANA), National Institute for Materials Science (NIMS), Tsukuba 305-0044, Japan

[∥]Elements Strategy Initiative for Catalysts and Batteries (ESICB), Kyoto University, Kyoto 615-8245, Japan

[⊥]Department of Chemistry, Faculty of Science, Hokkaido University, Sapporo 060-0810, Japan

Supporting Information

ABSTRACT: Boron nitride (BN), which is an insulator with a wide band gap, supported on Au is theoretically suggested and experimentally proved to act as an electrocatalyst for oxygen reduction reaction (ORR). Density-functional theory calculations show that the band gap of a free h-BN monolayer is 4.6 eV but a slight protrusion of the unoccupied BN states toward the Fermi level is observed if BN is supported on Au(111) due to the BN−Au interaction. A theoretically predicted metastable configuration of O_2 on h-BN/Au(111), which can serve as precursors for ORR, and free energy diagrams for ORR on h-BN/Au(111) via two- and four-electron pathways show that ORR to H_2O_2 is possible at this electrode. It is experimentally proved that overpotential for ORR at the gold electrode is significantly reduced by depositing BN nanosheets. No such effect is observed at the glassy carbon electrode, demonstrating the importance of BN−substrate interaction for h-BN to act as the ORR electrocatalyst. A possible role of the edge of the BN islands for ORR is also discussed.

Fuel cells (FCs) are considered to be one of the best possible energy conversion devices due to their high energy density, high theoretical efficiency, and negligible emission of exhaust gases.[1] The oxygen reduction reaction (ORR) has been extensively studied, as it is the most crucial process in FCs.[2−4] Pt based ORR electrocatalysts are widely used because of their relatively low overpotential.[5] However, due to the high cost, less abundance, poor stability in an electrochemical environment, and still sluggish kinetics of Pt based catalysts,[5−10] there are worldwide research efforts to find precious-metal-free catalysts, such as nonprecious metals,[6−11] their alloys or oxides,[12−15] and nitrogen-coordinated metals.[16,17] Recently metal-free carbon materials doped with N, B, P, and/or I,[18−26] particularly, N- and B-doped carbon materials, have been demonstrated to be effective precious-metal-free ORR catalysts. The enhanced ORR catalytic activity of N-doped carbon was attributed to the electron accepting nature of N-species, which creates a net positive charge on neighboring C atoms, where O_2 is adsorbed.[20,21] On the other hand, O_2 is considered to be adsorbed on the B atom itself in the case of B-doped carbon due to the electron accepting nature of the B atom.[23] A carbon electrode codoped with B and N atoms has higher ORR catalytic activity than that doped with a single element.[23−25] If all the C atoms in graphene are substituted by B and N atoms, a hexagonal boron nitride (h-BN) monolayer, which has a geometric structure similar to that of graphene, can be obtained. Actually we have recently shown theoretically that a N-doped h-BN monolayer can have electrocatalytic activity for ORR.[27,28] However, since BN is an insulator with a wide band gap (3.6−7.1 eV depending on experimental methods),[29,30] an electronic communication to the h-BN surface is essential for BN based materials to be used as an electrocatalyst for ORR.[27,28] Recently, manipulation of the band structure of h-BN nanosystems has attracted considerable interest because of possible applications of BN in nanoelectronics.[31] The band gap of the h-BN monolayer can be significantly reduced by B- and N-vacancies and impurity defects.[32,33] Moreover, the atomically thin h-BN nanoribbons are shown to possess semiconducting properties due to conducting edge states and vacancy defects.[32] More recently, electron tunneling through ultrathin h-BN layers deposited on a gold surface was demonstrated.[34] Therefore, ultrathin BN nanosheet (BNNS) layers supported on conducting materials may act as an ORR active electrocatalyst as necessary conditions seem to be fulfilled.

Theoretical calculations have demonstrated that the h-BN monolayer readily binds to the surface of various transition metals due to the mixing of the d_z^2 metal orbitals with the N-p_z and B-p_z orbitals of h-BN.[35] Such mixing is responsible for considerable modification of the electronic properties of the h-BN monolayer supported on 3d, 4d, and 5d transition metal surfaces[28,36] and also affects the catalytic activity of small metal particles supported on h-BN.[35,37] Recently, the possibility of functionalization of monolayer h-BN by the Ni(111) support for ORR has been demonstrated theoretically based on density

Received: January 14, 2014
Published: April 28, 2014

dx.doi.org/10.1021/ja500393g | J. Am. Chem. Soc. 2014, 136, 6542−6545

functional theory (DFT).[28] It has been shown that Ni(111) substrate can dramatically change the ability of h-BN to activate the O−O bond in O_2 and OOH species,[28] showing h-BN/Ni(111) is a good candidate as an ORR catalyst. Ni is, however, not stable in the potential region close to the onset of ORR and, therefore, not a good substrate to prove the theoretical suggestion of the electrocatalytic activity of BN for ORR. Thus, gold is selected as a substrate because of its high stability and low electrocatalytic activity for ORR in acidic solution.

Theoretical analysis of the electronic structure of the h-BN/Au(111) system and its ability to bind and activate the molecular oxygen were performed. The catalytic activation of O_2 is the first and one of the most important steps for ORR. The calculations are carried out based on DFT with the functional of Wu and Cohen.[38] The Au(111) surface is represented by the four-layer slab containing 7 × 7 unit cells of Au covered by the 8 × 8 element of h-BN. Calculations details are presented as Supporting Information (SI).[27,28]

It is demonstrated that h-BN monolayer weakly binds to the Au(111) surface with a binding energy of 0.06 eV per BN pair. Figure 1 shows the spin-polarized density of states (DOS)

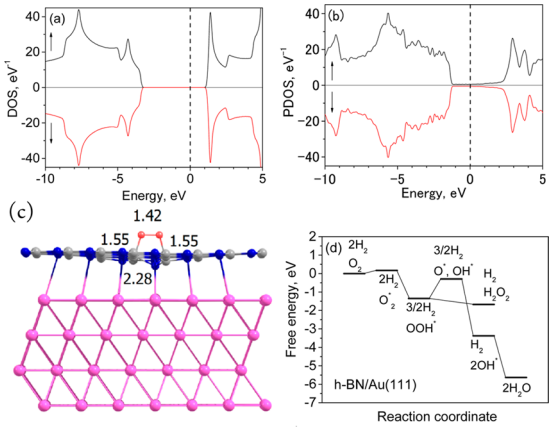

Figure 1. (a) Spin-polarized DOS calculated for the defect-free h-BN monolayer. (b) PDOS projected on B and N atoms for the h-BN/Au(111). The Fermi level is indicated by a dashed vertical line at 0 eV. Arrows directed upward and downward indicate the spin-up and spin-down DOS, respectively. (c) Optimized structure of the metastable O_2 on the h-BN/Au(111) surface with the distances given in angstrom. (d) Free energy diagram for ORR on the h-BN/Au(111).

calculated for (a) the free h-BN monolayer and (b) the h-BN monolayer supported on the Au(111) substrate. The calculation shows that the free h-BN monolayer has a wide band gap of 4.6 eV (Figure 1a), which is within the highly dispersed experimental values.[29,30] The calculated partial DOS (PDOS) of h-BN on Au(111) is slightly modified and a slight protrusion of the unoccupied BN states toward the Fermi level due to the interaction with Au is observed (Figure 1b). A similar but much stronger effect resulting in formation of the gap states has been observed experimentally for h-BN adsorbed on Ni(111), Rh(111), and Pt(111) surfaces[39] and explained by the orbital mixing and electron sharing at the interface.[36,39,40] Although O_2 can only physisorb on the h-BN/Au(111) in a triplet inactivated state similar to the adsorption on the unsupported h-BN, a metastable highly activated configuration of O_2 on h-BN/Au(111) with a binding energy of −0.05 eV is found, as shown in Figure 1c. In this case O_2 binds to two B atoms nearest to the N atom sitting on top of Au in the first metal layer. As a result of formation of the metastable O_2 on the h-BN/Au(111) surface, the h-BN monolayer is strongly deformed and bends toward the metal surface. Therefore, adsorption of O_2 on h-BN/Au(111) can promote the local bonding of h-BN with Au(111).

Free energy diagrams for ORR at the h-BN/Au(111) surface are obtained by accounting for entropy contribution, zero-point energy corrections, and solvent effects on the adsorption energies of O_2 and all ORR intermediates with the assumption of independent adsorption of ORR intermediates.[27,28] Two processes, i.e., a four-electron process via OOH producing water and a two-electron process producing H_2O_2, shown below where * denotes the adsorption site are considered, and results are summarized in Figure 1d.

(1) Four-electron process to water:

$$O_2 + * \rightarrow O_2^* \quad (1a)$$

$$O_2^* + (H^+ + e^-) \rightarrow OOH^* \quad (1b)$$

$$OOH^* \rightarrow O^* + OH^* \quad (1c)$$

$$O^* + (H^+ + e^-) \rightarrow OH^* \quad (1d)$$

$$2OH^* + 2(H^+ + e^-) \rightarrow 2H_2O \quad (1e)$$

(2) Two-electron process to hydrogen peroxide:

$$O_2 + * \rightarrow O_2^* \quad (2a)$$

$$O_2^* + (H^+ + e^-) \rightarrow OOH^* \quad (2b)$$

$$OOH^* + (H^+ + e^-) \rightarrow H_2O_2 \quad (2c)$$

It is clear that while the dissociation of OOH* to O* and OH* leading to the four-electron process is not energetically favorable, the reduction of OOH* to H_2O_2 is possible. It must be noted that dissociation of OOH* is energetically favorable at h-BN/Ni(111).[27,28] Unusually strong stabilization of OOH* can be explained by the large solvent effect. Detailed theoretical analysis of the ORR energetics for the BN/Au(111) system will be reported elsewhere.

Since the above-mentioned theoretical investigations suggest that BN on Au can act as an electrocatalyst for ORR, the ORR behavior of Au modified by BNNS, which was prepared by liquid exfoliation (see SI), was investigated.[41,42]

HRTEM images of the exfoliated BNNS (Figure 2) obtained by JEOL-JEM-2100F with power = 200 keV shows that BNNS are composed of single to a few layers with a honeycomb BN lattice. The fast Fourier transform (FFT) from the image (inset of Figure 2a) also indicates that BNNS are composed of a hexagonal atomic structure. Figure 2b shows the presence of zigzag and armchair edge structures. The chemical composition and structure of the exfoliated BNNS were determined by electron energy loss spectroscopy (EELS). The observed spectrum (Figure 2c) is similar to the previously reported EELS spectra and shows the characteristic K-edge absorptions of B- and N-atoms around 188−244 and 398−447 eV, respectively. A sharp peak followed by a wider band corresponding to 1s π^* and 1s σ^* transitions, respectively, is the characteristics of sp^2 hybridization, indicating the hexagonal arrangements of BNNS.[32]

Figure 3 shows the SEM images of the Au substrate (a) without and (b, c) with BNNS modification (see SI) using Hitachi, FE-SEM S-4800. BNNS were uniformly distributed

dx.doi.org/10.1021/ja500393g | J. Am. Chem. Soc. 2014, 136, 6542−6545

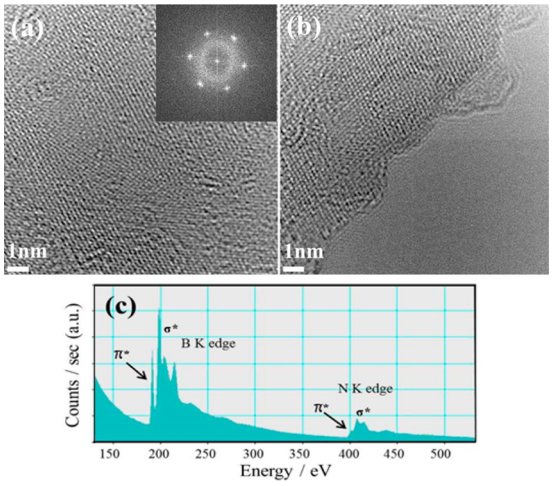

Figure 2. HRTEM images of (a) the center and (b) the edge of BNNS. Inset in (a) is the FFT pattern of single layer BNNS. (c) EELS spectrum of the exfoliated BNNS.

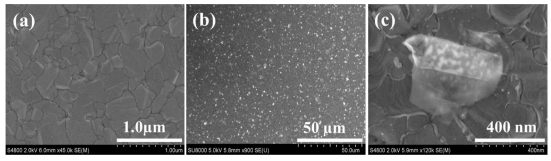

Figure 3. SEM images of (a) bare Au and (b,c) after exfoliated BNNS were deposited on the Au surface.

throughout the gold surface (Figure 3b). The size of exfoliated BNNS is on the order of a few hundreds of nm in the lateral dimension (Figure 3c). The peak position of the Raman spectrum of BNNS on Au suggests the presence of the monolayer (see SI).[43]

Figure 4 shows the linear sweep voltammograms (LSVs) of (i) bare and (ii) BNNS modified Au electrodes obtained in an O_2

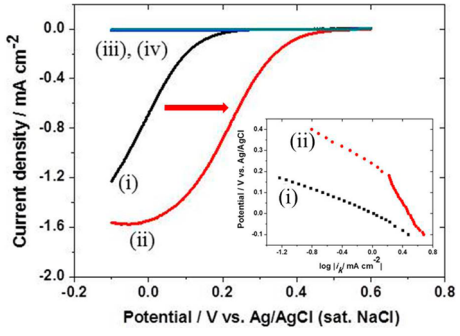

Figure 4. LSVs of (i) bare Au, (ii) BNNS/Au, (iii) bare GC, and (iv) BNNS/GC in O_2 saturated 0.5 M H_2SO_4. Rotation rate: 1500 rpm. Scan rate: 10 mV/s. Inset: Tafel plot of kinetic currents at (i) bare Au and (ii) BNNS/Au obtained by using K–L plot.

saturated 0.5 M H_2SO_4 solution in a rotating disk electrode configuration (Hokuto Denko, HR-202). The potential was scanned from +0.6 to −0.1 V. It is clear that BNNS acts as an electrocatalyst for ORR as the overpotential is reduced by ca. 0.27 V if BNNS is placed on Au. The number of electrons involved in ORR determined from the slope of Levich plot (limiting current vs $\omega^{1/2}$)[44] is ca. 2, showing the ORR product is H_2O_2, at both the bare and BNNS modified Au electrode. A rotating ring disk electrode study also showed that the current efficiency for H_2O_2 formation is almost 100% at both electrodes. Tafel plots of the kinetic currents at (i) bare and (ii) BNNS modified Au electrodes, which were obtained by analyzing the results of Figure 4 using the Koutecky–Levich (K–L) plot (current^{-1} vs $\omega^{-1/2}$),[44] give different slopes as shown in the inset of Figure 4, suggesting ORR proceeds with different mechanisms at these electrodes.

To examine the effect of the substrate, ORR behaviors of (iii) bare and (iv) BNNS modified glassy carbon (GC) electrodes were also measured under the same conditions used for Au electrodes. A GC substrate was chosen because theoretical calculation shows that graphite support does not affect electronic structure of the supported monolayer of h-BN and BNNS/graphite is not active for O_2 adsorption. In contrast to the results at the Au substrate, almost no electrocatalytic activity was observed at both the (iii) bare and (iv) BNNS modified GC electrode, confirming the important role of the Au substrate for the activation of BNNS for the ORR catalyst.

Now remains the question of where is the active site for ORR. The above calculations for O_2 adsorption and the free energy diagram are for the terrace of BNNS/Au, but the important role of the edge for O_2 adsorption at the N-doped carbon was suggested.[45] A current sensing AFM study (see SI) showed that the BNNS on Au was not very conductive even when the thickness of the BNNS was ∼0.9 nm, suggesting that the edge region of BNNS[46] is more favorable for ORR than the terrace. Thus, the adsorption of O_2 at the edge of h-BN islands of a finite size supported on the Au(111) surface was examined theoretically. As a simplest model for the h-BN island, we have considered the hydrogen terminated 3 × 3 element of the h-BN layer on Au(111), which is represented by a four-layer slab containing 8 × 8 unit cells of Au. It is demonstrated that O_2 can readily adsorb in highly activated states at the edges of the BN island in two different configurations as shown in Figure 5: (a)

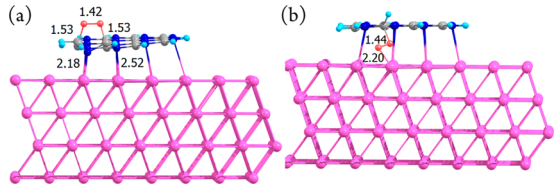

Figure 5. Optimized structures of O_2 adsorbed in (a) B–B bridge and (b) B–Au bridge configurations at the edge of the small h-BN island on the Au(111) surface. The distances are given in angstroms.

bridging two B atoms at the BN edge and (b) bridging B and Au atoms at the perimeter interface between the BN island and the Au(111) surface with binding energies of O_2 calculated for the B–B and B–Au bridge configurations of 0.4 and 0.2 eV, respectively, while adsorbed O_2 can exist only in a metastable configuration on defect-free BNNS monolayer on Au(111). This suggests the importance of the edge of BNNS as an ORR site, although more detailed experimental and theoretical investigations are required to define the actual reaction site. For example, a free energy diagram for ORR via edge adsorbed O_2 must be obtained and the reaction site must be detected in situ.

In conclusion, theoretical calculation suggested that activation of the adsorbed O_2 and a two-electron reduction pathway from O_2 to H_2O_2 are possible on BNNS/Au. The ORR activity of BNNS/Au was examined using a gold electrode modified by a single and few layers of BNNS. The overpotential for ORR was

dx.doi.org/10.1021/ja500393g | J. Am. Chem. Soc. 2014, 136, 6542–6545

reduced by BNNS modification by ca. 0.27 V, proving the theoretical suggestion. The interface between the BNNS and Au seems to play a vital role in the observed enhancement of the ORR activity. Although the present catalyst is not as active as Pt for ORR, the present combined theoretical and experimental study demonstrates the possibility to functionalize inert materials to become ORR catalyts, opening new ways to design effective Pt-free catalysts for FC based on materials never before considered as catalysts.

■ ASSOCIATED CONTENT

Supporting Information

Details of theoretical and experimental methods, and results of Raman scattering and AFM measurements. This material is available free of charge via the Internet at http://pubs.acs.org.

■ AUTHOR INFORMATION

Corresponding Author

Kohei.UOSAKI@nims.go.jp

Present Addresses

[¶]On leave from V. A. Fock Institute of Physics, St. Petersburg State University, 198504 St. Petersburg, Petrodvorez, Russia.
[+]Catalysis Research Center, Hokkaido University, Sapporo 001-0021, Japan.

Notes

The authors declare no competing financial interest.

■ ACKNOWLEDGMENTS

The present work was partially supported by Elements Science and Technology Project on "Nano-hybridized Precious-metal-free Catalysts for Chemical Energy Conversion", World Premier International Research Center (WPI) Initiative on Materials Nanoarchitectonics, the Development of Environmental Technology using Nanotechnology, and Elements Strategy Initiative for Catalysts & Batteries (ESICB) from the Ministry of Education, Culture, Sports, Science and Technology (MEXT), Japan.

■ REFERENCES

(1) Gasteiger, H. A.; Markovic, N. M. *Science* **2009**, *324*, 48.
(2) Shao, M. H.; Sasaki, K.; Adzic, R. R. *J. Am. Chem. Soc.* **2006**, *128*, 3526.
(3) Stamenkovic, V. R.; Fowler, B.; Mun, B. S.; Wang, G. F.; Ross, P. N.; Lucas, C. A.; Markovic, N. M. *Science* **2007**, *315*, 493.
(4) Yu, E. H.; Scott, K.; Reeve, R. W. *J. Electroanal. Chem.* **2003**, *547*, 17.
(5) Markovic, N. M.; Schmidt, T. J.; Stamenkovic, V.; Ross, P. N. *Fuel Cells* **2001**, *1*, 105.
(6) Winter, M.; Brodd, R. J. *Chem. Rev.* **2004**, *104*, 4245.
(7) Kongkanand, A.; Kuwabata, S.; Girishkumar, G.; Kamat, P. *Langmuir* **2006**, *22*, 2392.
(8) Zhang, J.; Sasaki, K.; Sutter, E.; Adzic, R. R. *Science* **2007**, *315*, 220.
(9) Lim, B.; Jiang, M. J.; Camargo, P. H. C.; Cho, E. C.; Tao, J.; Lu, X. M.; Zhu, Y. M.; Xia, Y. N. *Science* **2009**, *324*, 1302.
(10) Colmati, F.; Antolini, E.; Gonzalez, E. R. *J. Power Sources* **2006**, *157*, 98.
(11) Zhang, J.; Yang, H.; Fang, J.; Zou, S. *Nano Lett.* **2010**, *10*, 638.
(12) Chen, W.; Kim, J. M.; Sun, S. H.; Chen, S. W. *J. Phys. Chem. C* **2008**, *112*, 3891.
(13) Yu, X. W.; Ye, S. Y. *J. Power Sources* **2007**, *172*, 145.
(14) Shao, Y. Y.; Liu, J.; Wang, Y.; Lin, Y. H. *J. Mater. Chem.* **2009**, *19*, 46.
(15) Wang, Y. J.; Wilkinson, D. P.; Zhang, J. J. *Chem. Rev.* **2011**, *111*, 7625.
(16) Liu, R. L.; Wu, D. Q.; Feng, X. L.; Mullen, K. *Angew. Chem., Int. Ed.* **2010**, *49*, 2565.
(17) Wu, Z. S.; Yang, S. B.; Sun, Y.; Parvez, K.; Feng, X. L.; Mullen, K. *J. Am. Chem. Soc.* **2012**, *134*, 9082.
(18) Sidik, R. A.; Anderson, A. B.; Subramanian, N. P.; Kumaraguru, S. P.; Popov, B. N. *J. Phys. Chem. B* **2006**, *110*, 1787.
(19) Ozaki, J.-i.; Anahara, T.; Kimura, N.; Oya, A. *Carbon* **2006**, *44*, 3358.
(20) Gong, K. P.; Du, F.; Xia, Z. H.; Durstock, M.; Dai, L. M. *Science* **2009**, *323*, 760.
(21) Hu, X. B.; Wu, Y. T.; Li, H. R.; Zhang, Z. B. *J. Phys. Chem. C* **2010**, *114*, 9603.
(22) Wang, S. Y.; Iyyamperumal, E.; Roy, A.; Xue, Y. H.; Yu, D. S.; Dai, L. M. *Angew. Chem., Int. Ed.* **2011**, *50*, 11756.
(23) Zhao, Y.; Yang, L. J.; Chen, S.; Wang, X. Z.; Ma, Y. W.; Wu, Q.; Jiang, Y. F.; Qian, W. J.; Hu, Z. *J. Am. Chem. Soc.* **2013**, *135*, 1201.
(24) Yang, D. S.; Bhattacharjya, D.; Inamdar, S.; Park, J.; Yu, J. S. *J. Am. Chem. Soc.* **2012**, *134*, 16127.
(25) Ikeda, T.; Boero, M.; Huang, S.-H.; Terakura, K.; Oshima, M.; Ozaki, J.; Miyata, S. *J. Phys. Chem. C* **2010**, *114*, 8933.
(26) Yao, Z.; Nie, H. G.; Yang, Z.; Zhou, X. M.; Liu, Z.; Huang, S. M. *Chem. Commun.* **2012**, *48*, 1027.
(27) Lyalin, A.; Nakayama, A.; Uosaki, K.; Taketsugu, T. *Phys. Chem. Chem. Phys.* **2013**, *15*, 2809.
(28) Lyalin, A.; Nakayama, A.; Uosaki, K.; Taketsugu, T. *J. Phys. Chem. C* **2013**, *117*, 21359.
(29) Solozhenko, V. L.; Lazarenko, A. G.; Petitet, J. P.; Kanaev, A. V. *J. Phys. Chem. Solids* **2001**, *62*, 1331 and references therein.
(30) Golberg, D.; Bando, Y.; Huang, Y.; Terao, T.; Mitome, M.; Tang, C. C.; Zhi, C. Y. *ACS Nano* **2010**, *4*, 2979.
(31) Lin, Y.; Connell, J. W. *Nanoscale* **2012**, *4*, 6908.
(32) Zeng, H. B.; Zhi, C. Y.; Zhang, Z. H.; Wei, X. L.; Wang, X. B.; Guo, W. L.; Bando, Y.; Golberg, D. *Nano Lett.* **2010**, *10*, 5049.
(33) Azevedo, S.; Kaschny, J. R.; de Castilho, C. M. C.; Mota, F. D. *Eur. Phys. J. B* **2009**, *67*, 507.
(34) Britnell, L.; Gorbachev, R. V.; Jalil, R.; Belle, B. D.; Schedin, F.; Katsnelson, M. I.; Eaves, L.; Morozov, S. V.; Mayorov, A. S.; Peres, N. M. R.; Neto, A. H. C.; Leist, J.; Geim, A. K.; Ponomarenko, L. A.; Novoselov, K. S. *Nano Lett.* **2012**, *12*, 1707.
(35) Gao, M.; Lyalin, A.; Taketsugu, T. *Int. J. Quantum Chem.* **2013**, *113*, 443.
(36) Laskowski, R.; Blaha, P.; Schwarz, K. *Phys. Rev. B* **2008**, *78*, 045409.
(37) Gao, M.; Lyalin, A.; Taketsugu, T. *Catalysts* **2011**, *1*, 18; *J. Phys. Chem. C* **2012**, *116*, 9054; *J. Chem. Phys.* **2013**, *138*, 034701.
(38) Wu, Z. G.; Cohen, R. E. *Phys. Rev. B* **2006**, *73*, 235116.
(39) Preobrajenski, A. B.; Krasnikov, S. A.; Vinogradov, A. S.; Ng, M. L.; Kaambre, T.; Cafolla, A. A.; Martensson, N. *Phys. Rev. B* **2008**, *77*, 085421.
(40) Diaz, J. G.; Ding, Y.; Koitz, R.; Seitsonen, A. P.; Iannuzzi, M.; Hutter, J. *Theor. Chem. Acc.* **2013**, *132*, 1350.
(41) Nicolosi, V.; Chhowalla, M.; Kanatzidis, M. G.; Strano, M. S.; Coleman, J. N. *Science* **2013**, *340*, 6139.
(42) Han, W. Q.; Wu, L. J.; Zhu, Y. M.; Watanabe, K.; Taniguchi, T. *Appl. Phys. Lett.* **2008**, *93*, 223103.
(43) Gorbachev, R. V.; Riaz, I.; Nair, R. V.; Jalil, R.; Britnell, L.; Belle, B. D.; Hill, E. W.; Novoselov, K. S.; Watanabe, K.; Taniguchi, T.; Geim, A. K.; Blake, P. *Small* **2011**, *7*, 465.
(44) Bard, A. J.; Faulkner, L. R. *Electrochemical Methods: Fundamentals and Applications*, 2nd ed.; Wiley: New York, 2000.
(45) Ikeda, T.; Boero, M.; Huang, S.-H.; Terakura, K.; Oshima, M.; Ozaki, J. *J. Phys. Chem. C* **2008**, *112*, 14706.
(46) Alem, N.; Erni, R.; Kisielowski, C.; Rossell, M. D.; Gannett, W.; Zettl, A. *Phys. Rev. B* **2009**, *80*, 155425.